Barrier distributions of the ^{24}Mg + ^{90,92}Zr systems: Influence of energy dissipation

A. Trzcińska,[1,*] E. Piasecki,[1] G. Cardella,[2] D. Dell'Aquila,[3] E. De Filippo,[2] S. De Luca,[2,4] B. Gnoffo,[2,5] M. Kowalczyk,[1] G. Lanzalone,[6,7] I. Lombardo,[8] C. Maiolino,[6] N. S. Martorana,[6,5] A. Pagano,[2] E. V. Pagano,[6] S. Pirrone,[2] G. Politi,[2,5] L. Quattrocchi,[2,5] F. Rizzo,[6,5] P. Russotto,[6] A. Trifiro,[2,4] M. Trimarchi,[2,4] and M. Vigilante[8]

[1]*Heavy Ion Laboratory, University of Warsaw, Warsaw, Poland*
[2]*INFN–Sezione di Catania, Catania, Italy*
[3]*INFN–Sezone di Napoli and Dipartimento di Fisica Universitá di Napoli Federico II, Napoli, Italy*
[4]*Dipartimento di Scienze Matematiche e Informatiche, Scienze Fisiche e Scienze della Terra Universitá di Messina, Messina, Italy*
[5]*Dipartimento di fisica e astronomia Universitá di Catania, Catania, Italy*
[6]*INFN-LNS, Catania, Italy*
[7]*Facoltà di Ingegneria e Architettura, Universitá Kore, Enna, Italy*
[8]*INFN–Sezione di Napoli and Dipartimento di Fisica Universitá di Napoli Federico II, Napoli, Italy*

(Received 1 August 2019; revised 28 February 2020; accepted 30 July 2020; published 25 September 2020)

We present results of barrier distribution measurements for ^{24}Mg + ^{90,92}Zr systems by the backscattering method. The measurements were done at near-barrier beam energies of 68–88.5 MeV (in the laboratory frame) at six angles. A strong discrepancy between experimental results and the predictions of the standard coupled channels calculations was observed. To test the hypothesis that this discrepancy may be due to partial energy dissipation caused by coupling to many target noncollective levels, we performed calculations using the coupled channels plus random matrix theory (CC+RMT) model. The comparison of calculations with experimental results gives qualitative support of the hypothesis; however, quantitatively the agreement is not as good as in the case of the ^{20}Ne projectile.

DOI: 10.1103/PhysRevC.102.034617

I. INTRODUCTION

It is known that the kinetic energy of the relative motion between projectile and target can be partially dissipated into internal degrees of freedom of the nuclei. In the paper [1] we compared results of Coulomb barrier distribution D_{qe} measurements in the ^{20}Ne + ^{90,92}Zr and ^{20}Ne + ^{58,60,61}Ni systems [2,3], performed in the Heavy Ion Laboratory (University of Warsaw), with theoretical predictions. This comparison supports a hypothesis on the influence of dissipation on the Coulomb barrier tunneling. The study of this problem is important because the usual treatment of nuclear reactions as closed systems is only an approximation.

For the determination of D_{qe} we used the quasielastic backscattering method described in Ref. [4]. Its main idea consists in counting the number of the quasielastically scattered projectile nuclei by detectors set at backward angles and in monitors placed at forward angles. The latter ones register the Rutherford scattered ions. One can show that in an approximation [4] the barrier distribution (BD) can be obtained by determination of the ratio of the backward to forward scattering cross sections as a function of beam energy and calculation the first derivative of this dependence:

$$D_{qe}(E) \equiv -\frac{d}{dE}\left[\frac{\sigma_{qe}}{\sigma_{\mathrm{Ruth}}}(E)\right]. \quad (1)$$

It was shown in Ref. [4] that D_{qe} is approximately equivalent to the barrier distribution determined by the fusion method, D_{fus}, described in Ref. [5].

Theoretically, in Ref. [1], the problem of dissipation was treated using the CC+RMT model [6–8], constructed by merging the coupled channels (CC) method and the random matrix theory (RMT). Despite many approximations, quantitative agreement with experimental results for ^{20}Ne interacting with ^{90,92}Zr, and ^{58,60,61}Ni can be considered surprisingly good. Because this was obtained without fitting parameters for individual systems, the predictive power of the model is promising and should be checked with other systems.

In the present article we describe D_{qe} measurements performed for the systems ^{24}Mg + ^{90,92}Zr. According to the standard CC method, strong deformation of projectile nuclei should determine the structure of the barrier distributions, so the shape of BD should be very similar in the case of both targets. However, according to the tested model, the multitude of weak channels of single particle (s.p.) excitations should smooth out this structure when the target level density is high, as is the case of ^{92}Zr, while the structure should survive in the case of semimagic ^{90}Zr target, having much lower level density.

Preliminary results of the experiment were published in conference proceedings [9].

II. EXPERIMENT AND DATA ANALYSIS

The projectile ^{24}Mg was chosen because its structure is similar to ^{20}Ne, used in the previous experiments. While

*Corresponding author: agniecha@slcj.uw.edu.pl

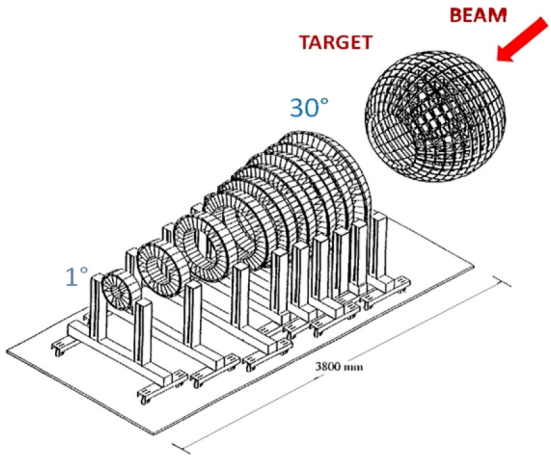

FIG. 1. CHIMERA multidetector system. The target was placed in the center of the sphere.

consisting of six α particles (instead of five in ^{20}Ne), it has also strong deformation, so the CC calculations predict significant structure in the barrier distribution. Besides, the $1n$ and $2n$ transfer Q_{gg} values are small or negative, so we expected that the cross sections for these reactions should be small thus they should not play an important role in the shape of the BD. It was experimentally checked in separate experiments that the cross sections for transfer channels are small. Preliminary results have been published in conference proceedings [10].

In the reported experiment a ^{24}Mg beam of $\approx$50 e nA intensity, accelerated to energies spanning the 68–88 MeV range in 0.5 MeV steps, was delivered by the Tandem MP of the LNS INFN (Catania). We used ^{90}Zr (enriched to 98%) and ^{92}Zr (94%) targets of 100 μg/cm^2 thickness, prepared from ZrO_2 on a C backing of 30 μg/cm^2 thickness. The target thickness was the main source of the 0.6 MeV energy uncertainty [FWHM in the center-of-mass (c.m.) frame], which was, however, much smaller than the width of the expected structures. Because of this, even if taken into account, its influence on the D_{qe} shape was negligible. The scattered Mg ions were registered using the multidetector CHIMERA system [11]; see Fig. 1.

Backscattered ions were registered by rings of Si detectors placed in the sphere at six backward angles: 122°, 130°, 138°, 146°, 159.5°, and 169.5° in the laboratory system (135°, 142°, 148°, 154.5°, 162.5°, and 172.5° in the c.m. frame). The angular resolution ±4° resulted in ±0.2 MeV (c.m. frame) energy uncertainty of backscattered ions. Four detectors placed at forward angles (29°), where Rutherford scattering dominates, measured $\sigma_{\rm Ruth}$ and were also used to monitor the beam energy.

The method of data analysis is described in Refs. [2,12]. Briefly, the energy spectra of registered ions were transformed to the Q-value spectra assuming two-body kinematics; see formula (5) in Ref. [12]. The number of counts was determined by integrating the system excitation energy (Q-value) spectra in the wide window $-5 < -Q < 20$ MeV. This procedure enabled us to reject the background events. After binning over 0.3 MeV intervals, the excitation function $\sigma_{qe}/\sigma_{\rm Ruth}(E_{\rm eff})$ was

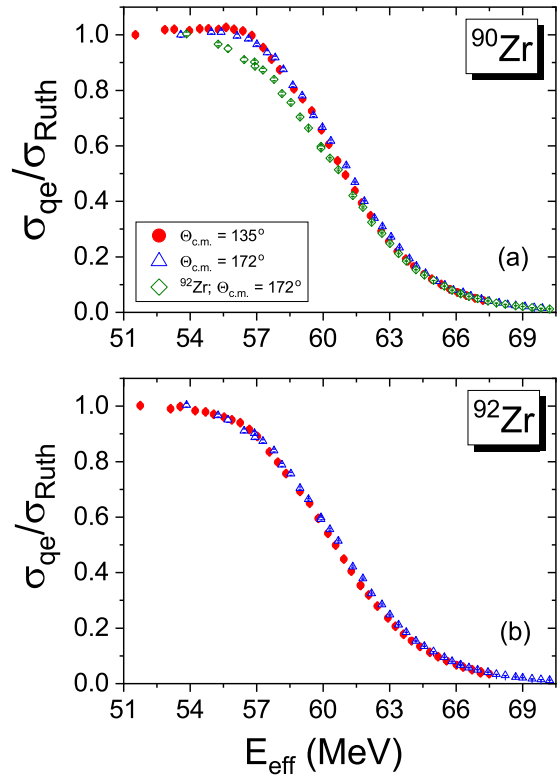

FIG. 2. Excitation functions for quasielastic backscattering of ^{24}Mg on ^{90}Zr (a) and ^{92}Zr (b) measured at 135° (red circles) and 172° (blue triangles) in the center-of-mass system. Error bars are smaller than the data symbols. In the (a) panel the results obtained at 172° for ^{92}Zr target are also shown (in green diamonds) for comparison between ^{90}Zr and ^{92}Zr targets.

constructed, where $E_{\rm eff}$ took into account the angle-dependent centrifugal energy [4,13,14] by the formula

$$E_{\rm eff} = \frac{2E_{\rm c.m.}\sin(\theta_{\rm c.m.}/2)}{1+\sin(\theta_{\rm c.m.}/2)}. \quad (2)$$

Then the data were normalized by imposing $\sigma_{qe}/\sigma_{\rm Ruth}$ at the lowest energy equal to 1.0. In this way, precise knowledge of the detector solid angles, the target thickness, and the absolute beam current was not necessary, so related systematic errors were avoided.

III. EXPERIMENTAL RESULTS

In Fig. 2 we present examples of the quasielastic backscattering excitation functions for the smallest and largest scattering angles used in measurements. For the intermediate angles, results are similar. We present there also the comparison of excitation functions for both targets.

Differences between results obtained for the two Zr isotopes are seen much better after the differentiation of the excitation functions [Eq. (1)]. In Fig. 3 the experimental BDs simultaneously measured in the same conditions at six angles are shown together. The figure shows, in agreement with our expectations, that the barrier distribution of ^{24}Mg + ^{90}Zr has a clear structure, while in the case of ^{92}Zr the structure is completely washed out.

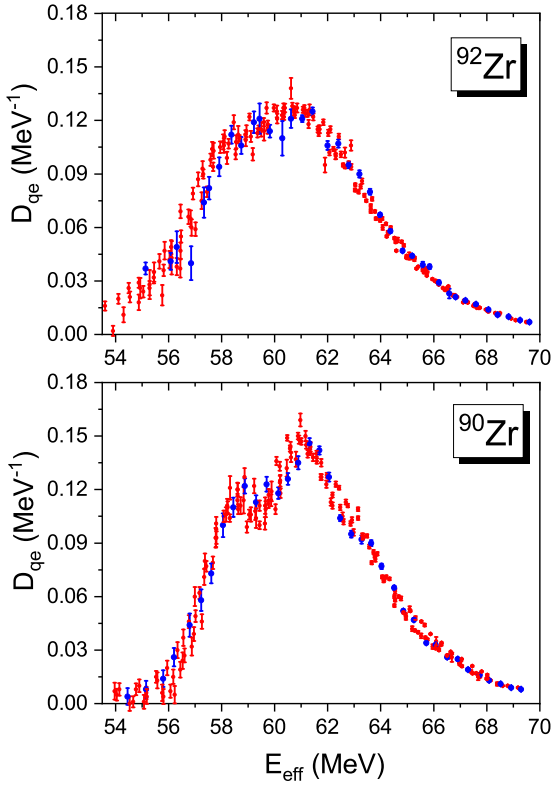

FIG. 3. D_{qe} of ^{24}Mg interacting with the ^{90,92}Zr targets. The data from all six measurement angles, without any binning, are shown together. The data for 169.5° in the laboratory system are plotted with the blue points to identify the most backward angle data, where the quasielastic barrier distribution is expected to be closest to the barrier distribution determined by the fusion method.

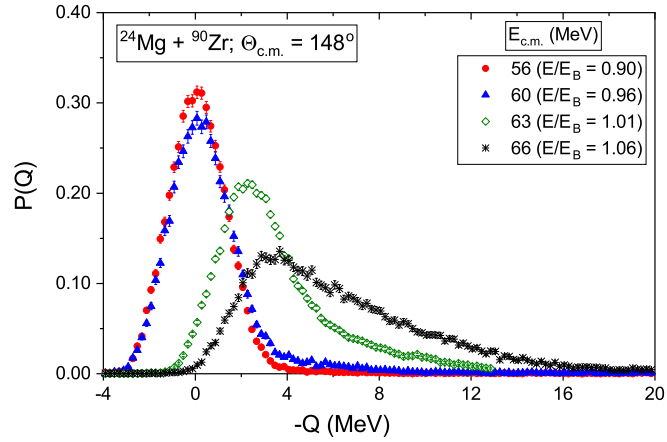

FIG. 4. Examples of dissipation (excitation energy) distributions of the system ^{24}Mg + ^{90}Zr measured at c.m. angle 148° for four projectile energies. E/E_B is the ratio of the the projectile energy to single barrier energy 62.2 MeV [15]. For better visualization, the area of distributions is normalized to 1.0. The negative values of $-Q$ are due to the energy resolution.

As we mentioned above, the target thickness did not influence the D_{qe} shape; however, it did influence the backscattered projectile energy. As a result, the uncertainty of the system excitation energy (Q value) shown in Fig. 4 was pretty large, ≈3 MeV FWHM in the c.m. frame, and was slightly energy and angle dependent. However, this did not influence our results because during data analysis we needed only to put the wide window on this spectrum. Anyhow, the Q-value window dependence of D_{qe} is very weak (see Sec. VI).

Due to experimental possibilities of the CHIMERA detection system, we were able to measure simultaneously barrier distributions for wider angular range and at a larger number of angles than in our previous experiments, and we found that especially for smaller angles their angular dependence is significant (Figs. 5 and 6), which is seen especially well for the ^{90}Zr target. This means that the scaling, given by Eq. (2), is not sufficient for the description of D_{qe} angular dependence, as in reality it concerns not only the energy shift [as suggests Eq. (2)] but also the shape of the distribution.

We stress that, since the first papers on D_{qe} distributions, the formula (2) was in general use, even if we are not aware of any systematic experimental verification of this correction. While it is certainly good as the first approximation, especially for angles close to 180°, already in earlier papers we noticed that its precision depends on the system under study. For example, while it worked well for ^{20}Ne + ^{90,92}Zr [2] and ^{20}Ne + ^{58,60,61}Ni [3], in paper [16] we noticed that for the ^{20}Ne + ^{208}Pb system Eq. (2) was not sufficient, so barrier distributions for three angles were presented there separately.

The reason why the scaling [Eq. (2)] is not good enough is that to compute $E_{\rm eff}$ one uses the classical approximation of the Coulomb trajectory, disregarding any quantal effects due to the nuclear potential [4]. As a result, we get only the shift of D_{qe} along the energy axis. In reality, it is obvious that different angles mean different impact parameters and that at some distance the nuclear interaction comes into play. We are aware of only one attempt to go beyond the simplest approximation: the paper of Diaz-Torres *et al.* [17]. We tried to apply Eq. (2) of this paper, but it turned out that the results were practically indistinguishable from that obtained by the standard correction of Ref. [4]. The reason is that also the formula of the paper [17] describes only the energy shift, while in reality we should include here the effects of couplings to the excited states. These couplings would change the classical trajectory after the state is excited, as the relative energy will be changed. Since the excitation probability of any level depends on the angle, by changing observation angle one can observe changes in the barrier structure generated by coupling to the levels. This is seen both in experimental results as well as in the CC calculations of D_{qe} including the dissipation effects, as we show in Sec. V.

IV. CC+RMT MODEL CALCULATIONS

According to our hypothesis [2], for the ^{20}Ne + ^{90,92}Zr systems, the BD structure, generated by couplings to collective excitations (mainly) in the projectile, is at least partly smoothed out by couplings to the target s.p. excitations, the density of which in ^{92}Zr is much higher than in ^{90}Zr (and even more than in the projectile). To check this hypothesis quantitatively, for the ^{24}Mg + ^{90,92}Zr systems we performed theoretical calculations in the frame of the CC+RMT model,

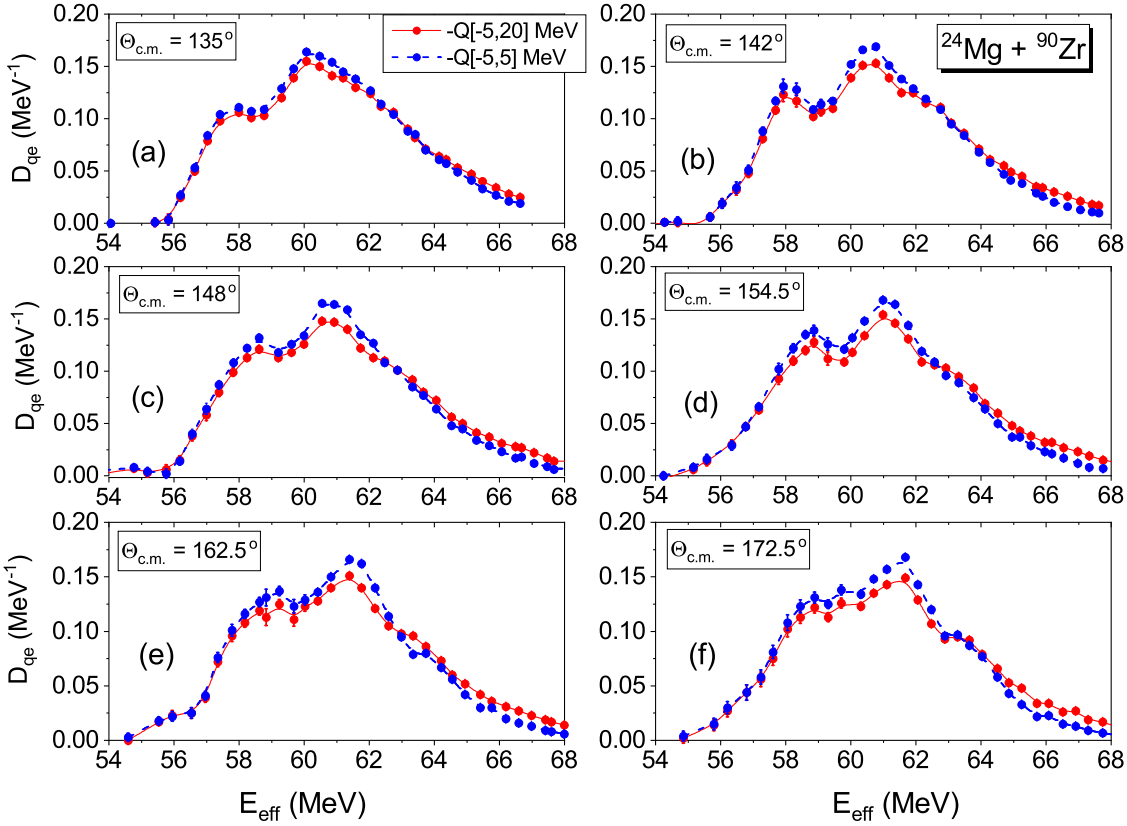

FIG. 5. Experimental barrier distributions for ^{24}Mg + ^{90}Zr obtained for narrow and wide Q-value windows presented for all measurement angles.

described in Refs. [1,6–8]. As in the cases ^{20}Ne + ^{90,92}Zr and ^{58,60,61}Ni [1] we did not fit any model parameters for individual systems, taking them from external sources. For the real part of the potentials, we assumed the Woods-Saxon (WS) shape with parameters V, r_{ov}, and a_v of the Akyuz-Winther potential [15]. The imaginary part of the potential, of the WS form, was assumed to be well localized inside the barrier, to ascertain internal absorption after tunneling. In our application, with this assumption, the precise values of W, r_{ow}, and a_w (for which we have assumed 30 MeV, 0.9 fm, and 0.5 fm, respectively) have a very weak influence on the results. The radius parameter for the couplings is set in all cases to 1.20 fm.

The values for the other parameters, taken from Refs. [18–20], are shown in Table I. The number of phonons/rotational states shown in Table I was sufficient to get convergence of the results.

The key factor in the CC+RMT approach is the level density $\rho(E)$, where E is the excitation energy. In the present calculations, as in Ref. [1], for the theoretical level densities we employ the results of Skyrme-Hartree-Fock-Bogoliubov (HFB) calculations by Goriely *et al.* [23,24].

V. RESULTS OF THE CALCULATIONS

Using the CC+RMT model one can observe how strong is the influence of coupling to the single particle levels on the barrier distribution D_{qe}. The comparisons of experimental barrier distributions with calculated ones are presented in Figs. 7 and 8. The theoretical predictions shown there were calculated without dissipation and with dissipation switched on by including couplings to 150 s.p. levels. It is worthwhile to pay attention to the fact that theoretical predictions without dissipations are very similar for both systems while the experimental results differ significantly. The evolution of D_{qe} with the rising number of included noncollective levels is shown in Fig. 9.

Because the shapes of BDs are angle dependent (Fig. 10), for a more quantitative comparison of experiment and model results for ^{24}Mg + ^{90,92}Zr, in Figs. 7 and 8 we compare for each measurement angle separately.

As we stressed in Ref. [1], since we are more interested here in the shapes than the absolute positions of BD, the theoretical curves calculated taking into account dissipation were normalized to the experimental distributions in the peaks, and also shifted to higher energy by 0.6 MeV for ^{90}Zr and 1.5 MeV for ^{92}Zr targets. If we include the noncollective excitations, in principle, we would have to change the potential parameters to reproduce the experimental data, e.g., changing the r_{ov} parameter from 1.175 fm to 1.15 fm. However, we do not want to fit any parameters to have some predictive possibilities. In general, the coupling to states with large excitation energy leads to a shift of the potential barrier [1,21,22].

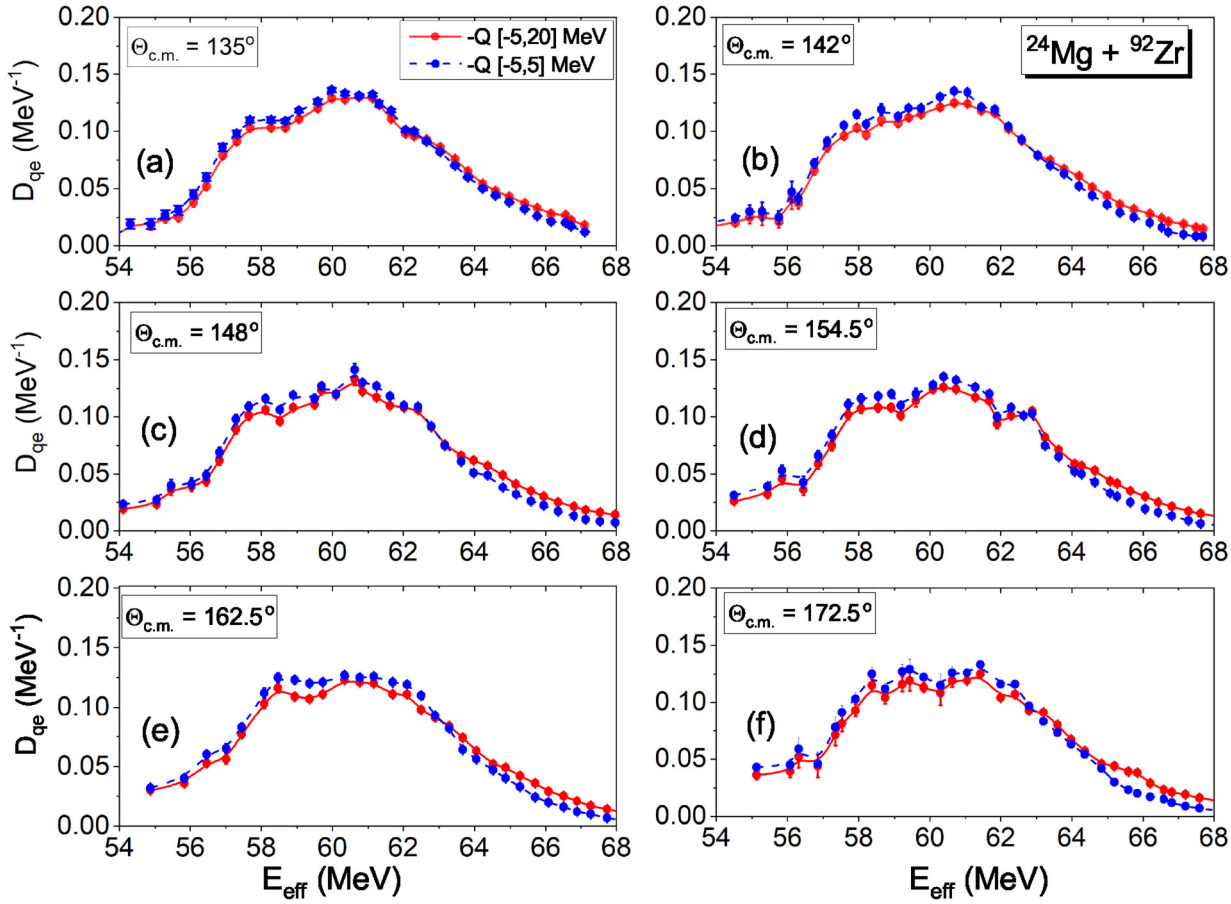

FIG. 6. Experimental barrier distributions for ^{24}Mg + ^{92}Zr obtained for narrow and wide Q-value windows presented for all measurement angles.

From the Figs. 7 and 8 one can see that

(1) Calculations taking into account collective excitations only give rise to very wide barrier distributions with clearly three or even four maxima for both targets, while experimentally two maxima for the ^{90}Zr target and only one for the ^{92}Zr target are observed.
(2) As we expected, dissipation, i.e., excitation of s.p. levels, smoothes out the barrier distribution much less for the ^{90}Zr target than in the ^{92}Zr case. Consequently, the lower energy hump (at about 58 MeV), seen in experimental data for the ^{90}Zr target, is seen also in the calculated distributions.
(3) For the ^{92}Zr target, the dissipation completely smoothes out the structures in the calculated barrier distributions; however, the treatment of dissipation in the frame of the CC+RMT model causes too strong distribution narrowing.

TABLE I. The parameters used in the coupled-channels calculations. For the ^{24}Mg projectile nucleus, only the rotational excitations of the ground state rotational band are included. The high energy 3^- vibrational level in the projectile nucleus was omitted since it causes only the adiabatic potential renormalization [21,22].

	^{24}Mg	^{90}Zr	^{92}Zr
$E(2^+)$ (MeV)	(rot.) 1.369	(vib.) 2.18	(vib.) 0.93
β_2 (β_4)	0.59 (−0.03)	0.089	0.1027
The number of phonons/rotational states	3	1	1
$E(3^-)$ vib. (MeV)	7.616	2.75	2.34
β_3	0.27	0.211	0.17
The number of phonons	0	1	1
V (MeV)		64.5	64.8
r_{ov} (fm)		1.175	1.175
a_v (fm)		0.65	0.65

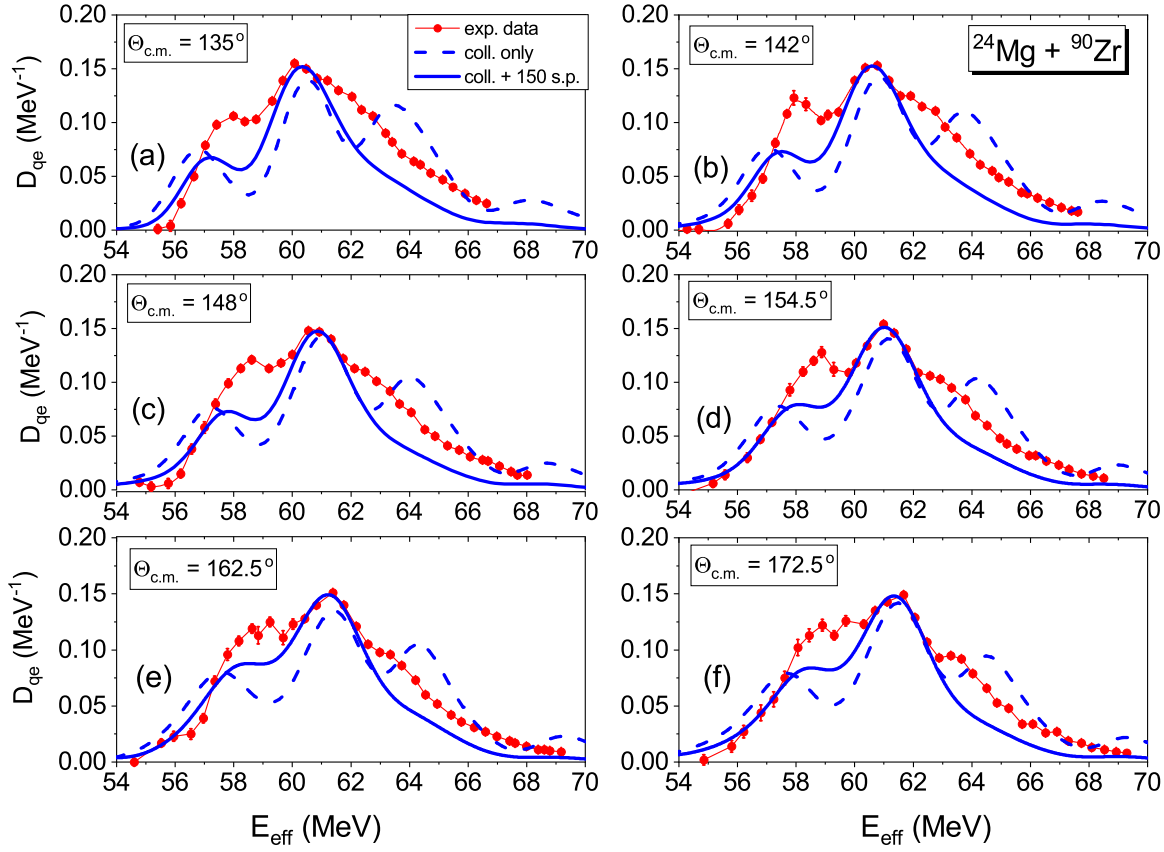

FIG. 7. Comparison of experimental barrier distributions for ^{24}Mg + ^{90}Zr (red points connected by red lines for better visibility) with calculated results without dissipation (dashed blue lines) and with dissipation switched on by including couplings to 150 s.p. levels (solid blue lines). The experimental energy resolution was taken into account.

VI. DISCUSSION

We are aware of only one measurement of the ^{24}Mg + ^{90}Zr barrier distribution [25]. According to that article, the measured D_{qe} has no trace of any structure. The reason for disagreement between that work and our results is not known. The theoretical description in that article was obtained by using the standard (no-dissipation) CCQEL code. Fitting the β_2 and β_4 deformation parameters, the authors obtained values significantly different from the ones used by us in the calculations. The target isotope dependence of the BD observed experimentally, which is not reproduced by CC calculations taking into account only collective excitations, points to some deficiency of the model. Can the smoothing of the BD structure be caused by coupling to transfer channels, usually not taken into account by the model? This is still an open question due to difficulties concerning the fully quantal transfer calculations (for a discussion of various approaches see Refs. [26–28] and references therein). According to the model described in Ref. [26], it is expected that transfer influences fusion mainly via $1n$ and $2n$ channels, and it should be significant mainly when the ground-state-to-ground-state Q value, Q_{gg}, for these channels is positive. In cases with $Q_{gg} < 0$ it is assumed that transfer may be disregarded. Because of this assumption the model cannot explain our results concerning D_{qe} for ^{20}Ne + ^{58,60,61}Ni, since for all three systems $Q_{gg} < 0$ for the most probable transfer channels. On the other hand, according to a series of papers of Sargsyan *et al.*, [29,30], the transfers can either enhance or hinder the fusion cross sections, depending on the deformation change of the participating nuclei after transfer, but before fusion or scattering. However, since in their model excitations to collective states are not considered, the barrier distribution structures are not expected at all. Still, the structure was observed in many systems.

Concerning the relation between dissipation and modification of BDs, one should note that in quasielastic scattering, where the elastic flux is the main part of the scattered one, the cross section can be strongly affected by the couplings to collective and noncollective levels in the moment of interaction. However, afterward one cannot remove their action by applying the corresponding excitation energy windows. This is illustrated in Fig. 11, showing results of calculations concerning the ^{24}Mg + ^{90}Zr system. To simplify interpretation, the calculation was performed without dissipation and with the assumption that the ^{90}Zr target is inert (i.e., without excitations). We took into account only rotational excited states of ^{24}Mg at 1.369, 4.563, and 9.583 MeV. It is seen that removing the second and third excited states by applying the Q-value window $0 < -Q < 1.5$ MeV influences the BD only marginally, while removing them from the CC scheme changes the barrier distribution radically. The

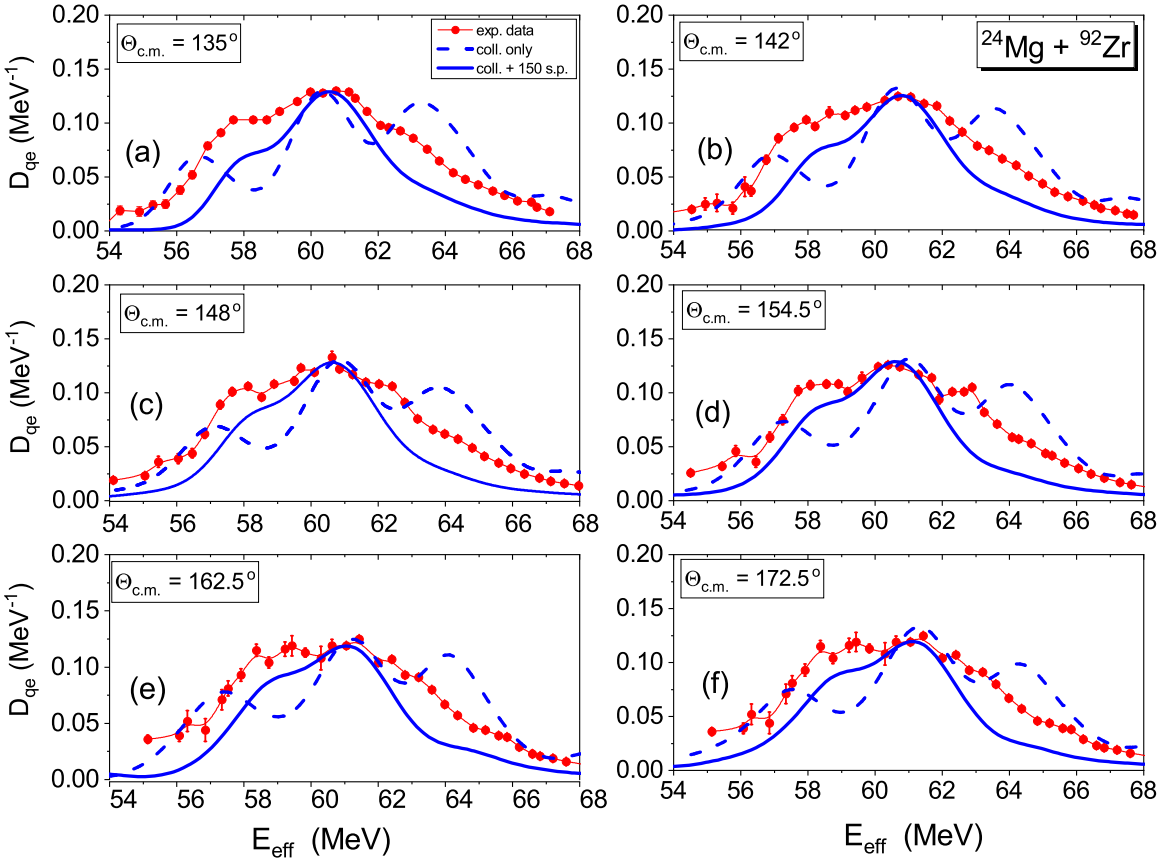

FIG. 8. The same as in Fig. 7 for the ^{92}Zr target.

same applies also to noncollective excitations. This explains why the barrier experimental distributions in the quasielastic scattering studied in this article are almost independent of the Q-value window; see Figs. 5 and 6. As shown there, the Q-value window dependence of D_{qe} is very weak. The small modification above the barrier can be understood by looking at experimental Q-value distributions shown for few projectile energies in Fig. 4 and at the dependence of the quasielastic excitation function on the Q-value window width; see Fig. 12. For beam energies up to the barrier, the Q values are close to 0, meaning (almost) elastic scattering. Only for energies above the barrier structure does the

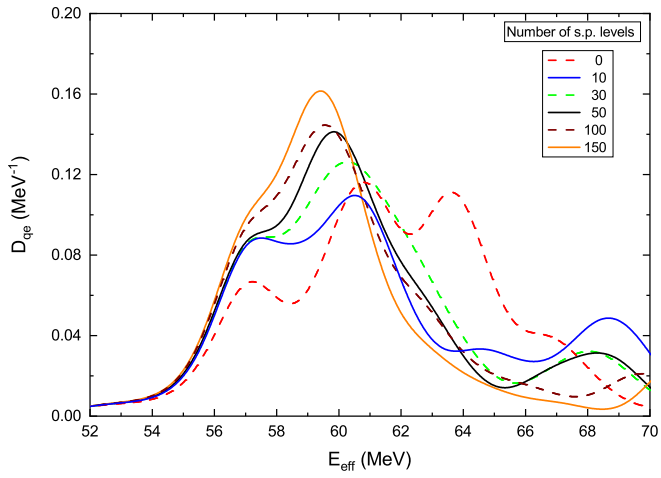

FIG. 9. Evolution of D_{qe} shapes calculated for various numbers of single particle levels (in addition to the collective ones) for the ^{24}Mg + ^{92}Zr system at $\Theta_{\text{c.m.}} = 154^{\circ}$. Maximal excitation energies of the target nucleus are 2.0, 2.9, 3.3, 3.9, and 4.2 MeV for 10, 30, 50, 100, and 150 s.p. levels, respectively.

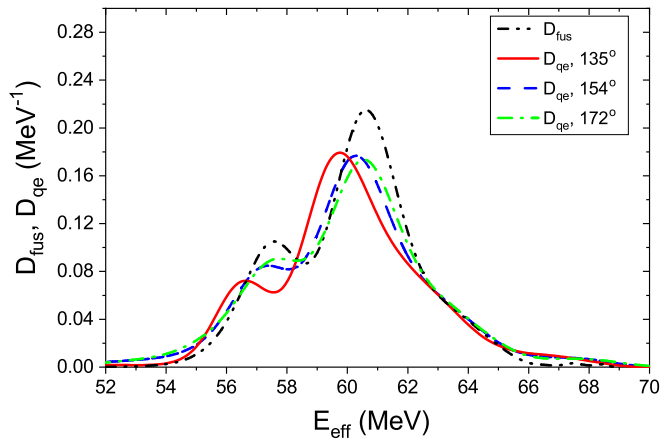

FIG. 10. D_{qe} for ^{24}Mg + ^{90}Zr calculated for three angles in the c.m. frame taking into account 150 s.p. level excitations. For comparison, D_{fus}, calculated with the same input parameters, is also presented.

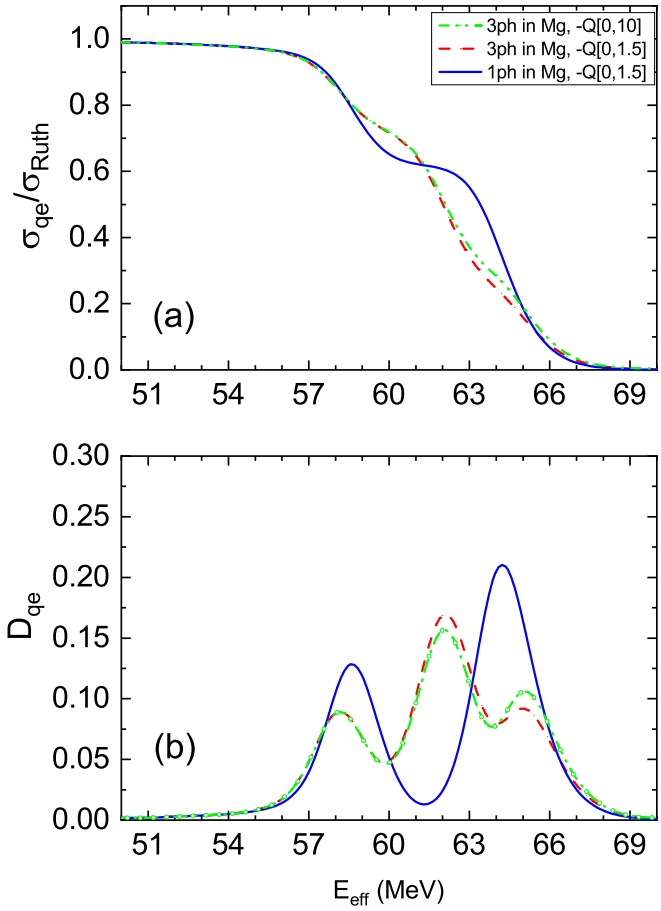

FIG. 11. Excitation function (a) and barrier distribution (b) for the ^{24}Mg + ^{90}Zr system calculated for the inert target and including excitations in the projectile: one phonon excitation (solid line), three phonons (dashed-dotted line), and three phonons after selecting the data in the narrow Q-value window (dashed line).

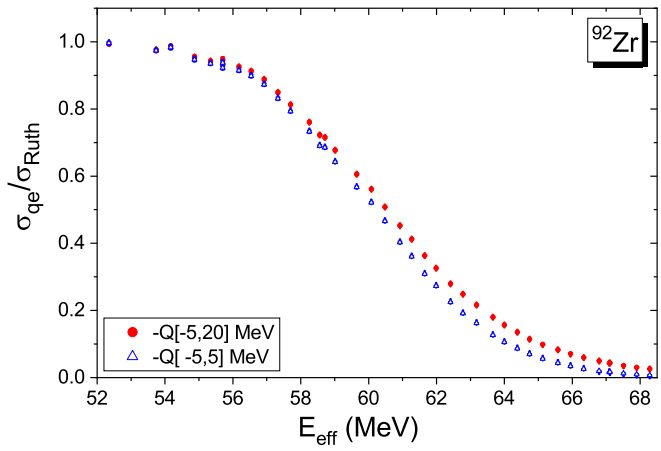

FIG. 12. Example of influence of the Q-value window on the quasielastic scattering excitation function for ^{24}Mg + ^{92}Zr, measured at 142° (c.m. frame). For the ^{90}Zr target and other angles, the influence is similar.

Q-value distribution start to shift and extend to higher values. Consequently, by narrowing the Q-value window we reject only some events from the high-energy part of the excitation function (Fig. 12), weakly changing the high energy tail of the BD.

Our experimental results, as well as the CC+RMT model calculations, qualitatively agree with the hypothesis claiming the significant influence of dissipation (caused by couplings to s.p. levels) on D_{qe} barrier distributions. However, at the quantitative level, there are some problems. Namely, for the ^{20}Ne projectile [1] the width of experimental barrier distribution is equal to 6.1 MeV (FWHM), while for ^{24}Mg the FWHM is larger, equal to 7.1 MeV, in agreement with expectation, according to which the width of the barrier distribution should be approximately proportional to $Z_{proj}Z_{targ}$ (see Eq. (17) in Ref. [31]). However, while the theoretical D_{qe} width for the ^{20}Ne projectile equals 6.0 MeV, the one for ^{24}Mg is too narrow: only 4.8 MeV, in significant disagreement with the experimental result. Narrowing due to the couplings to s.p. levels is notsurprising per se, as the density of noncollective levels is strongly rising with energy, so these couplings are dominated by high energy excitations. This, in turn, gives rise to narrowing and shifting down barrier distributions due to the adiabatic potential renormalization [6,21]; however, the cause of quantitative disagreement with the experiment is for the moment not clear.

In Ref. [1] we enumerated a list of assumptions and approximations of the CC+RMT model. The list is long, so it is still difficult to pinpoint the single reason for too strong narrowing of the calculated distributions caused by dissipation (especially for the ^{92}Zr target) which was not observed in the case of the ^{20}Ne beam [1]. Since in both cases the targets were the same, the cause should be attributed to the projectile structure.

It is known that the BD structures are essentially determined by couplings to collective levels. According to our calculations, couplings to statistical noncollective levels tend only to efface these structures. On the other hand Yusa in Ref. [32] proved within the first-order perturbative approximation that narrowing of the peak tends to occur when rotational coupling associated with prolate deformation is present. In this context, one should notice that the β_2 deformation of ^{24}Mg is significantly larger than of the ^{20}Ne nucleus (0.59 vs 0.46). Moreover, we have checked that in the ^{20}Ne case the dissipation did not cause so strong D_{qe} shrinkage due to the β_4 deformation, which in the ^{24}Mg nucleus is almost absent (-0.03 vs 0.27 in ^{20}Ne). Both effects, however, are taken into account in the CC+RMT model, so the reason for the overnarrowing of BD in the case of ^{24}Mg should be rather looked for in some collective properties of the projectile not taken here into account. One of them is the known nonaxiality, or more precisely the softness of this nucleus on deformation γ, which for the moment is not included in the CCRMT code.

Experimental information and experience with the model are still too limited to answer the question of whether the stationary CC+RMT model after some improvements can be sufficient to describe dissipation effects on tunneling, or perhaps one should go beyond the model in the spirit of ideas proposed in the papers of Diaz-Torres and collaborators

[33,34]. The answer to this important question requires further experimental and theoretical works.

VII. CONCLUSIONS

Concerning the influence of dissipation, we got the qualitative support of our hypothesis: the BD structure turned out to be visible in the ^{90}Zr and washed out in the ^{92}Zr target cases. Calculations using the CC+RMT model qualitatively agree with this observation: the partial energy dissipation, caused by the coupling of relative motion of the projectile and target nuclei to many s.p. excitations, is more than enough to explain the experimentally observed structure smoothing. However, the calculated barrier distributions are visibly too narrow in comparison with experiment, although the agreement is much better than without taking into account the partial energy dissipation.

We determined barrier distributions by measuring quasielastic ^{24}Mg + ^{90,92}Zr backscattering at six angles. It was demonstrated that the standard recipe of taking the observation angle into account by the transformation from projectile energy to the effective energy $E_{\rm eff}$ is not always sufficient to explain the shifts of D_{qe}, especially for angles far from 180°. Moreover, it turned out that not only the shift but also the shape of BD can be angle dependent.

Finally, results of the experiment support the conclusion of Ref. [1] that the determination of physical parameters by fitting them without taking into account weakly coupled channels may be questionable for medium and heavy systems, as the limited model space can strongly influence the fitting results.

ACKNOWLEDGMENTS

We are grateful to Kouichi Hagino for valuable discussions and suggestions. We thank also Kirby Kemper, Oleg Ponkratenko, Giulia Colucci, and Magda Zielińska for helpful comments. The authors are grateful to the LNS technical staff for providing both ^{24}Mg beam and ^{90,92}Zr targets of high quality. We are also thankful to the tandem crew for the smooth operation of the accelerator during the experiment. We would like to thank C. J. Lin and Y. Zhang for help with performing part of the CC+RMT calculations on the CIAE TH-1 supercomputer. This work was partly supported by the Polish National Science Centre under Contracts No. UMO-2013/08/M/ST2/00257 and No. UMO-2014/14/M/ST2/00738. This research was supported in part by the PL-Grid Infrastructure and the Interdisciplinary Centre for Mathematical and Computational Modelling (ICM), University of Warsaw, under Grant No. GB77-2.

[1] E. Piasecki, M. Kowalczyk, S. Yusa, A. Trzcińska, and K. Hagino, Phys. Rev. C **100**, 014616 (2019).
[2] E. Piasecki, Ł. Świderski, W. Gawlikowicz, J. Jastrzębski, N. Keeley, M. Kisieliński, S. Kliczewski, A. Kordyasz, M. Kowalczyk, S. Khlebnikov, E. Koshchiy, E. Kozulin, T. Krogulski, T. Loktev, M. Mutterer, K. Piasecki, A. Piórkowska, K. Rusek, A. Staudt, M. Sillanpää, S. Smirnov, I. Strojek, G. Tiourin, W. H. Trzaska, A. Trzcińska, K. Hagino, and N. Rowley, Phys. Rev. C **80**, 054613 (2009).
[3] A. Trzcińska, E. Piasecki, K. Hagino, W. Czarnacki, P. Decowski, N. Keeley, M. Kisieliński, P. Koczoń, A. Kordyasz, E. Koshchiy, M. Kowalczyk, B. Lommel, A. Stolarz, I. Strojek, and K. Zerva, Phys. Rev. C **92**, 034619 (2015).
[4] H. Timmers, J. R. Leigh, M. Dasgupta, D. J. Hinde, R. C. Lemmon, J. C. Mein, C. R. Morton, J. O. Netwon, and N. Rowley, Nucl. Phys. A **584**, 190 (1995).
[5] N. Rowley, G. R. Satchler, and P. H. Stelson, Phys. Lett. B **254**, 25 (1991).
[6] S. Yusa, K. Hagino, and N. Rowley, Phys. Rev C **82**, 024606 (2010).
[7] S. Yusa, K. Hagino, and N. Rowley, Phys. Rev. C **88**, 044620 (2013).
[8] S. Yusa, K. Hagino, and N. Rowley, Phys. Rev. C **88**, 054621 (2013).
[9] A. Trzcińska, E. Piasecki, M. Kowalczyk, G. Cardella, E. D. Filippo, D. Dell'aquila, S. D. Luca, B. Gnoffo, G. Lanzalone, I. Lombardo, C. Maiolino, N. Martorana, S. Norella, A. Pagano, E. V. Pagano, M. Papa, S. Pirrone, G. Politi, L. Quattrocchi, F. Rizzo, P. Russotto, A. Trifiro, M. Trimarchi, and M. Vigilante, Acta Phys. Pol. B **49**, 393 (2018).
[10] D. Wójcik, A. Trzcińska, E. Piasecki, M. Kisieliński, M. Kowalczyk, M. Wolińska-Cichocka, C. Bordeanu, B. Gnoffo, H. Jia, C. Lin, N. S. Martorana, M. Mutterer, E. V. Pagano, K. Piasecki, P. Russotto, L. Quatrocchi, W. H. Trzaska, G. Tiurin, R. Wolski, and H. Zhang, Acta Phys. Pol. B **49**, 387 (2018).
[11] A. Pagano, M. Alderighi, F. Amorini, A. A. L. Arena, L. Auditore, V. Baran, M. Bartolucci, I. Berceanu, J. Blicharska, J. Brzychczyk, A. Bonasera, B. Borderie, R. Bougault, M. Bruno, G. Cardella, S. Cavallaro, M. B. Chatterjee, A. Chbihi, J. Cibor, M. Colonna *et al.*, Nucl. Phys. A **734**, 504 (2004).
[12] E. Piasecki, M. Kowalczyk, K. Piasecki, Ł. Świderski, J. Srebrny, M. Witecki, F. Carstoiu, W. Czarnacki, K. Rusek, J. Iwanicki, J. Jastrzębski, M. Kisieliński, A. Kordyasz, A. Stolarz, J. Tys, T. Krogulski, and N. Rowley, Phys. Rev. C **65**, 054611 (2002).
[13] L. F. Canto, P. R. S. Gomes, R. Donangeloa, and M. S. Hussein, Phys. Rep. **424**, 1 (2006).
[14] K. Hagino and N. Rowley, Phys. Rev. C **69**, 054610 (2004).
[15] O. Akyüz and A. Winther, Nuclear structure and heavy-ion collisions, in *Proceedings of the International School of Physics "Enrico Fermi," Varenna, Italy, 1979*, edited by R. A. Broglia, C. H. Dasso, and R. Ricci (North-Holland, Amsterdam, 1981).
[16] E. Piasecki, Ł. Świderski, N. Keeley, M. Kisieliński, M. Kowalczyk, S. Khlebnikov, T. Krogulski, K. Piasecki, G. Tiourin, M. Sillanpää, W. H. Trzaska, and A. Trzcińska, Phys. Rev. C **85**, 054608 (2012).
[17] A. Diaz-Torres, G. Adamian, V. Sargsyan, and N. Antonenko, Phys. Lett. B **739**, 348 (2014).
[18] G. S. Blanpied, B. G. Ritchie,, M. L. Barlett, R. W. Fergerson, G. W. Hoffmann, J. A. McGill, and B. H. Wildenthal, Phys. Rev. C **38**, 2180 (1988).
[19] S. Raman, At. Data Nucl. Data Tables **78**, 1 (2001).

[20] R. H. Spear, At. Data Nucl. Data Tables **42**, 55 (1998).
[21] K. Hagino and N. Takigawa, Prog. Theor. Phys. **128**, 1061 (2012).
[22] K. Hagino, N. Takigawa, M. Dasgupta, D. J. Hinde, and J. R. Leigh, Phys. Rev. Lett. **79**, 2014 (1997).
[23] S. Goriely, S. Hilaire, and A. J. Koning, Phys. Rev. C **78**, 064307 (2008).
[24] http://www.talys.eu/documentation/.
[25] Y. Gupta, B. Nayak, U. Garg, K. Hagino, K. Howard, N. Sensharma, M. Senyigit, W. Tan, P. O'Malley, M. Smith, R. Gandhi, T. Anderson, R. deBoer, B. Frentz, A. Gyurjinyan, O. Hall, M. Hall, J. Hu, E. Lamere, Q. Liu, A. Long, W. Lu, S. Lyons, K. Ostdiek, C. Seymour, M. Skulski, and B. V. Kolk, Phys. Lett. B **806**, 135473 (2020).
[26] A. V. Karpov, V. A. Rachkov, and V. V. Samarin, Phys. Rev. C **92**, 064603 (2015).
[27] C. J. Lin, H. M. Jia, H. Q. Zhang, X. X. Xu, X. F. Yang, X. L. Yang, P. F. Bao, L. J. Sun, and Z. H. Liu, EPJ Web Conf. **63**, 02007 (2013).
[28] D. C. Rafferty, M. Dasgupta, D. J. Hinde, C. Simenel, E. C. Simpson, E. Williams, I. P. Carter, K. J. Cook, D. H. Luong, S. D. McNeil, K. Ramachandran, K. Vo-Phuoc, and A. Wakhle, Phys. Rev. C **94**, 024607 (2016).
[29] V. V. Sargsyan, G. G. Adamian, N. V. Antonenko, W. Scheid, and H. Q. Zhang, Phys. Rev. C **91**, 014613 (2015).
[30] V. V. Sargsyan, G. G. Adamian, N. V. Antonenko, W. Scheid, and H. Q. Zhang, Phys. Rev. C **95**, 054619 (2017).
[31] M. Dasgupta, D. J. Hinde, N. Rowley, and A. M. Stefanini, Annu. Rev. Nucl. Part. Sci. **48**, 401 (1998).
[32] S. Yusa, Ph.D. thesis, Tohoku University, 2013 (unpublished).
[33] A. Diaz-Torres, Phys. Rev. C **82**, 054617 (2010).
[34] A. Diaz-Torres, Phys. Rev. C **81**, 041603(R) (2010).